Supernatural Inflation:Inflation from Supersymmetry with No (Very) Small Parameters

by

Marin Soljačić

SUBMITTED TO THE DEPARTMENT OF PHYSICS IN PARTIAL FULFILLMENT OF THE REQUIREMENTS FOR THE DEGREE OF

BACHELOR OF SCIENCE IN PHYSICS
AT THE
MASSACHUSETTS INSTITUTE OF TECHNOLOGY

JUNE 1996

Signature of Author: _____

Department of Physics
May 10, 1996

Certified by: _____

Lisa J. Randall
Associate Professor of Physics
Thesis Supervisor

Approved by: _____

June L. Matthews
Professor of Physics
Department of Physics Undergraduate Thesis Coordinator

Supernatural Inflation:Inflation from Supersymmetry with No (Very) Small Parameters

by
Marin Soljačić

May 10, 1996

Submitted to the Department of Physics
on May 10, 1996 in Partial Fulfillment of the
Requirements for the Degree of Bachelor of Science in
Physics

Abstract

Most models of inflation incorporate small inexplainable parameters that do not exist normally in particle physics theories. We designed a model that avoids this; it implements inflation using only the parameters that already exist in the particle physics theories. We succeeded this by using two coupled quantum fields instead of using only one as it is usually done.

Using more fields than just one makes the model more complicated, and the analysis is harder. The proper analysis of the predictions of our model would therefore be purely numerical. However, as we show, the approximate analytical expressions we obtain are in an excellent agreement with the exact numerical solutions. Therefore, we use them to analyze and calculate its predictions.

Thesis Supervisor: Lisa J. Randall
Title: Associate Professor of Physics

Contents

List of Figures

Note: *Following a long tradition in Cosmology, we set all the constants k_B, c, and $\hbar$ to 1 throughout this paper. They are easy to reintroduce later on the basis of dimensional analysis.*

For a general review of the subject of inflationary cosmology, please refer to [2].

1 Big-Bang

Starting in the beginning of this century, many characteristics of the observable universe lead scientists to a conclusion that universe was created in a big explosion some 10-20 billion years ago. Therefore, all the energy of the universe was once concentrated in a very small volume of enormous temperature and energy density. This is the essence of the so-called the Hot Big-Bang model of the creation of the universe.

An important thing to realize about the idea that the whole universe evolved from a small volume, is that we are not talking about a purely three dimensional explosion, like the explosion of a bomb. A feature of an explosion which happens in a three dimensional space is that it has a well defined origin at which the explosion happened. In contrast, the "explosion" of the universe does not have such a three dimensional origin.

Instead the explosion happens in what we can picture to be four dimensions. The universe is like a three dimensional surface of a four dimensional balloon that is being blown. As the volume of the balloon increases, any two points on its surface move away from each other; the points that are further away move apart faster. In reality, this picture is slightly more complicated since we are not sure yet whether the universe is really like a "balloon" or like a four dimensional hyperbola; nevertheless, the essence of the description is the same.

1.1 Justification of Big-Bang model

In 1920, it was discovered that all observable stars are moving away from the solar system. This fact was detected by measuring the radiation spectrum of the stars, and observing that the further away a star was from us, the bigger red doppler shift its spectrum had. The red doppler shift meant of course that the star was moving away from us. Of the 28000 galaxy spectra

measured by the present day, a red shift was observed in all except a very few closest galaxies. This universal expansion was in a direct accord with the Big-Bang model.

If we are to believe the Hot Big-Bang model, we should expect that at the earliest stages of the development of the universe, all the particle species are in a thermal equilibrium with each other; that is, the whole universe was in a thermal equilibrium. To solve for the energy in each particle species, and the energy distribution of particles of each particle species, we can use the "black body" model, but with many more degrees of freedom than the black body we usually talk about; each particle species represents a degree of freedom in which the energy can be stored. Since all particles are relativistic at temperatures this high, the energy distribution of particles in each particle species will be the same as for a black body.

However, as the universe adiabatically expands, it cools down, the density of each species decreases, and the collisions between the particles needed to keep the universe in a thermal equilibrium become rare. Depending on the scattering cross section of a particular species, one after the other, particle species decouple from the thermal equilibrium. Nevertheless, at the moment of the decoupling, each species still has the energy distribution which follows from the black body model of the temperature at the time of the decoupling. After the decoupling, this energy redshifts due to the expansion of the universe. It turns out that the red-shift does not destroy the shape of the energy distribution; the only thing it does is to decrease the effective "temperature" the distribution is at. Consequently, we expect to observe some background photon radiation still present from the time of the creation of the universe. And, indeed, a cosmic microwave background radiation (**CMBR**) with the energy distribution of a black body at temperature of 2.726K is readily observed [1].

There is many other evidence that supports the Hot Big-Bang model; among the most important is light-element abundances, which are very difficult to explain without employing the Hot Big-Bang model. Consequently, the Hot Big-Bang model is universally accepted today, and it is used to make predictions about the state of the universe all the way to 0.01 sec after the bang.

1.2 The problems of the old Big-Bang model

In the recent decades, scientists began to realize significant disadvantages of the old Big Bang model. In fact, Collins and Hawking [8] showed that the set of initial data needed for the universe to evolve into a universe similar to ours is of measure zero. I summarize in this section many of the problems of the old the Big-Bang model. For a comprehensive discussion, please see [2].

1.2.1 The problem of the domain walls

In the beginning, the universe is at a very high temperature. Consequently, the term $\approx \phi^2 T^2$ which appears in the potentials of all fields dominates the potentials; and, all fields (except the ones which are very weakly coupled, so the temperature coupling is small) are confined to the origin.

However, as the temperature decreases, this term vanishes, and the fields are free to move to their true minimum. This can happen either through rolling towards the minimum, if there are no barriers between the origin and the true minimum, or through quantum tunneling if the barriers exist. But, there are many fields in particle physics theories which have more than one true minimum. For example, this could be a scalar field which has a *cos* potential. In this particular case, the field can roll either to the minimum on the left, or to the minimum on the right. In any case, the symmetry is broken.

There is no reason for a field to move to the same minimum in two causally disconnected regions of the universe. However, if it does not, a domain wall is created between the two regions. Many regions which were causally disconnected a long time in the past are within the observable universe today. So, we expect that there should be many domain walls present in the observable universe. Unfortunately, it turns out that a single domain wall in the entire universe would have energy density too high, and lead to unacceptable cosmological consequences [2].

1.2.2 The monopole problem

Besides the domain walls which can conceivably be created as a result of spontaneous symmetry breakings, most grand unified theories predict that magnetic monopoles could also be created. These monopoles are extremely heavy, and they decay very slowly. Zeldovich and Khlopov [2] showed that

magnetic monopole density in the observable universe should, therefore, be comparable to the baryon density; the energy density of the universe would be 10^{15} times higher than it is today, and the universe would have collapsed a long time ago.

1.2.3 The baryon asymmetry

The most anti-matter existing today is the one which is created in the high-energy colliders. There is no reason in principle that the whole universe has to be composed from matter instead from anti-matter (in fact, we could not tell the difference at all, and would probably be calling anti-matter to be matter today, and vice versa.) Due to the symmetry between the two, it is hard to conceive why the two are not present in same abundances. And while some clever philosophical attempts have been made to solve this problem, none of them explains why the ratio of baryons to photons is exactly as small as 10^{-9}.

1.2.4 The horizon problem

As we mentioned, the cosmic microwave background radiation has a temperature of 2.726K. This temperature is universal across the whole universe, with only small deviations of ± 0.01K. The observable universe today encompasses about 10^6 regions which were causally disconnected at the time of the CMBR decoupling. The fact that the CMBR is the same across the whole observable universe is therefore hardly explainable within the framework of the old the Big-Bang theory.

1.2.5 The flatness of space

This is one of the biggest problems of the old theory. It can be formulated in several ways, but the essence of the problem is that the only natural length scale in general relativity is the Planck length $l_P \approx 10^{-35}m$. The fact that the universe is flat on all observable scales, instead of being curved on the order of l_P is therefore a complete mystery to the old theory.

1.2.6 Other problems, and the solution

There are some other problems with the old Big Bang model, including: the problem of large-scale homogeneity, the galaxy formation problem, the gravitino problem, the problem of Polonyi fields, and the vacuum energy problem. However, in 1981, Professor Alan Guth [6] proposed the concept of inflation. Inflation, if implemented correctly, solves all of these problems except the vacuum energy problem. Consequently, inflation is a universally accepted theory today.

2 Inflation

The old Big Bang model provides a reliable account for the development of the universe from $0.01sec$ from the Big Bang till today. Its only problem is that the set of initial parameters at $t = 0.01sec$ needed for the universe to evolve to a universe qualitatively similar to ours is extremely unlikely. So, it is desirable to develop an upgrade on the theory which would explain how come the initial conditions were so special.

A very interesting philosophical idea was proposed in order to solve some of the problems. It is called the *anthropic principle*: "Unless the Universe and the laws of physics were as they are, intelligent life could not have developed to discover and discuss them." And, while it is true that some of the initial conditions indeed had to be special so that life could develop, the *anthropic principle* does not solve many of the problems; for example, it explains nothing about the uniformity of CMBR across the sky.

On the other hand, the concept of inflation, a purely scientific concept, solves all the problems except the vacuum energy problem; starting from almost any initial conditions, provided they allow for inflation to happen, many models of inflation exist that naturally predict a universe similar to ours.

2.1 How does inflation do it?

The basic idea of inflation is that there was a time interval in a region of the universe when the dominant component of the energy was the vacuum energy. According to the Friedmann equation, the scale factor R, then grows exponentially.

To see this, we write the Friedmann equation

$$\frac{\dot{R}^2}{R^2} + \frac{k}{R^2} = \frac{8\pi G}{3}\rho \ , \tag{1}$$

where $k = 1$ corresponds to a closed universe, $k = 0$ to a flat universe, and $k = -1$ to an open universe. Now, in the case when ρ is constant, this is solvable exactly; but, we can save ourselves some effort. It is clear that R grows faster and faster. As it grows, the term proportional to k becomes vanishingly small, and we are left with a pure exponential expansion of R. The $ln(R_{final}/R_{initial})$ is called the number of e-folds.

Consequently, a patch which was very small before inflation, and therefore very smooth can grow to be bigger than the region which will evolve into the observable universe today. Furthermore, the energy density of the relics existing before inflation drops to almost zero. However, during inflation, the entropy in the patch is fixed, and the temperature drops to zero. We now need a mechanism to reheat the universe; i.e. since we assumed the patch was small, the initial entropy in the patch was small also. As the patch encompasses the whole observable universe today, we want to increase the entropy in the patch. For this to happen, we allow the vacuum energy to decay into radiation once inflation ends. But, since the initial conditions for the decay are uniform across the patch, this decay will not cause new inhomogeneities across the patch.

If implemented correctly, inflation dilutes the magnetic monopoles, and inflates the domain walls created before inflation well out of the observable universe today. Furthermore, it explains the uniformity of CMBR. In addition, the radius of curvature of space, which is proportional to R grows enormously, thereby solving the flatness of space problem. Inflation also solves all the problems we did not elaborate on, except the vacuum energy problem. However, described the way we did it, it is not clear how inflation solves the small-scale inhomogeneity problem, or the baryon asymmetry problem; but, it turns out that the small-scale inhomogeneity can be solved through a correct implementation of inflation, while baryongenesis can be solved without contradicting inflation. We will elaborate on the issue of the small-scale inhomogeneity below, and concerning the issue of baryongenesis, we refer the reader to Section 9 of our paper [3].

2.1.1 Small-scale inhomogeneity

Every workable model of inflation has a mechanism that at a certain moment transforms the vacuum energy responsible for inflating the universe into matter or radiation energy, thereby stopping inflation, and reheating the universe. We argued above that the inflated patch stays smooth during inflation, because it was smooth in the beginning. But, the quantum fluctuations, of the fields responsible for inflation cause inflation to end at different times in different parts of the universe; this causes inhomogeneities across the universe.

These inhomogeneities manifest themselves in non-uniformities of the

CMBR temperature across the sky which was observed by the Cosmic Background Explorer (COBE) satellite [7]. It is believed that precisely these initial inhomogeneities evolved into the small-scale anisotropy we see today; indeed according to computer simulations, exactly the magnitude of the CMBR temperature anisotropies observed today corresponds to the magnitude of the initial perturbations needed to result in the observed structure of the universe today [4, 5, 7].

3 Existing models of inflation and our goal

In his revolutionary paper in which he introduced the concept of inflation, Prof. Guth also proposed the first model of inflation. It turned out later that the particular model he proposed did not work. Consequently, many cosmologists came up with their own models of inflation, and there are many workable models of inflation today. Unfortunately, there is not enough data yet, so we can not decide on the correct model.

Nevertheless, most models of inflation include very small parameters; this is necessary to get enough e-folds, while at the same time producing the density perturbations of the correct magnitude. There are already existing small inexplainable parameters in particle physics theories at many places. For example, we mention the ratio of the weak scale to the Planck scale, and the magnitude of the Yukawa coupling of the electron. However, introducing new inexplainable parameters whose only motivation is to implement inflation correctly weakens the credibility of a theory. Our goal in this project was therefore to develop a model of inflation which follows naturally from particle physics theories, using only the scales already present in the particle physics theories, and without including any new inexplainable parameters.

4 Our models

The essential idea behind our models is that we use two quantum fields instead of only one to implement inflation. This gives us more freedom in designing the model. We used this opportunity well, and succeeded to design a model that does not require any new small parameters.

The first field which we call ϕ, has a local maximum at the origin, and its true minimum is far away from the origin; it is on the order of M_P. The value of the potential in ϕ, when $\phi = 0$, provides the vacuum energy density needed for inflation. The potential of the other field ψ, has only a term $\propto {m_\psi}^2\psi^2$. Since m_ψ is small compared to H, the potential in ψ is naturally flat, and ψ slow-rolls towards the origin. It is the slow roll of this field that provides the required number of e-folds.

However, there is an additional coupling term between ψ and ϕ in the potential, which causes ϕ to have a huge mass at the origin when ψ is large. So, we start of with $\phi \approx 0$, and ψ large. After many e-folds, when ψ becomes small enough, the coupling term is not dominant for $m_\phi(t)$ any more, and ϕ is free to drop into its true minimum. Now, as ϕ becomes large, the mass of ψ grows enormously due to the coupling term, and ψ gets to the origin very quickly, beginning its coherent oscillations. Here, a third field, χ, which is coupled to ψ enters the scenario; all the energy leaks from ψ into χ very quickly, and we can forget about ψ from this point onwards.

Soon ϕ gets to its true minimum starting its coherent oscillations; this energy in ϕ eventually reheats the universe [3] since it turns out that the energy stored in χ at the moment of the reheating is many orders of magnitude smaller than the energy in ϕ [3].

We actually have two models, with two different coupling terms, and the equations of their potentials are as follows

$$V = M^4 \cos^2\left(\frac{\phi}{\sqrt{2}f}\right) + \frac{m_\psi^2}{2}\psi^2 + \frac{\psi^4\phi^2 + \phi^4\psi^2}{8M'^2} \tag{2}$$

from now on referred as to M' model, and,

$$V = M^4 \cos^2\left(\frac{\phi}{\sqrt{2}f}\right) + \frac{m_\psi^2}{2}\psi^2 + \frac{\lambda^2\psi^2\phi^2}{4}\ , \tag{3}$$

referred to as λ model.

Since ψ is the factor that holds ϕ at its false vacuum state for many e-folds, we avoided the need to tune the potential in ϕ; ψ acts like a switch to end inflation, so the shape of the potential in ϕ is almost irrelevant for obtaining enough e-folds, while the chosen shape of the potential in ψ is actually the most natural potential to expect. As we will see later, the required density perturbations are formed in a natural way, also.

4.1 Where do our models come from?

Our models follow from supersymmetric theories. So, it is to be expected that the scale M appearing in the models should be of the order M_I; for an explanation why this is so, please see [3].

As mentioned above, the particular shape of the potential in ϕ is almost irrelevant. This can be seen from the Taylor expansion of the potential; only at the very late stages of inflation are the terms higher than the constant and the mass term relevant, so their particular choice does not make much difference in the model at all. We chose the particular cos^2 shape because of its simplicity to think about.

By Taylor expansion of the potential in ϕ we see that the imaginary $m_\phi \equiv M^2/f$ at the origin. We expect that $f \approx M_P$, or equivalently $m_\phi \approx m_W$. According to the rules of supersymmetric theories, the shape of the potential in ϕ is as natural as they get. The most natural value to expect for m_ψ is $\approx m_W$ also, so this is the value we pick for m_ψ.

The only terms in the potentials (2) and (3) which we did not justify yet are the coupling terms. In fact, the coupling terms are the only terms where the two potentials differ. So, we justify the coupling terms now.

The coupling term in the M' potential is derived from a superpotential

$$W = \frac{\phi^2 \psi^2}{2M'} \ . \tag{4}$$

.

Our model is motivated by the properties of moduli fields, or flat directions of the standard model [3]. For the standard model flat directions, M' could conceivably be equal to M_P, M_G, or M_I. We explore all these possibilities later. To derive the potential from W, we write

$$V = \sum_i \left| \frac{\partial W}{\partial \xi_i} \right|^2 , \tag{5}$$

where ξ_is are all the fields appearing in W.

Since we are taking the scalar fields to be real, we put an additional factor of 1/8 to finally get the coupling term

$$\frac{\psi^4 \phi^2 + \phi^4 \psi^2}{8 M'^2} . \tag{6}$$

In the second type of the coupling we explore, we assume a superpotential of the form

$$W = \lambda \phi \psi \theta . \tag{7}$$

So, after using (5), and adding an additional factor of 1/4 to account for the fact that we take the scalar fields to be real, we get the final form of our coupling term to be:

$$\frac{\lambda^2 \psi^2 \phi^2}{4} . \tag{8}$$

This is so because we take $\langle \theta^2 \rangle \equiv 0$ so the other terms in V evaluate to zero. The coupling in (8) is a typical Yukawa coupling. Therefore, we assume $\lambda = 10^{-4}$.

4.2 Density perturbations

As discussed before, inflation predicts an extremely isotropic universe; all anisotropies are inflated away. Now, fortunately for us, although the universe seems very isotropic at the large scales, it is not perfectly isotropic at small scales. Unless inflation had a way to make up for this fact, we would have to abandon inflationary theory.

Inflation in fact does have a mechanism to predict some density perturbations. The basic idea is that although the evolution of the $\langle \psi \rangle$ can be described with the classical equations of motion, the development of ψ is not perfectly classical; there are some small quantum fluctuations of ψ around $\langle \psi \rangle$. These fluctuations cause inflation to end at slightly different times in

different parts of the universe thereby providing for the initial energy density perturbations.

As the time evolves, these, initially small perturbations are amplified through the gravitational, and some other effects, to result in the small scale anisotropies observed today. The magnitude of these initial perturbations can be readily calculated for any particular inflationary model: once it is calculated, it has to be compared with the density perturbations calculated from the CMBR anisotropies as explained above. Finally, the model has to be designed in such a manner as to predict the same density perturbations as the ones calculated from the CMBR.

Now, we calculate what density perturbations are predicted by our models. The equation derived from the CMBR anisotropies is given in [4, 5] for the slow-roll regime:

$$\frac{V^{3/2}}{\left[\left(M_P/\sqrt{8\pi}\right)^3 \left(\partial V/\partial\psi\right)\right]} = 6 \times 10^{-4} \ . \tag{9}$$

After a few lines of algebra, this gives us the following constraint for the M' model:

$$\frac{M^5}{m_\psi^2 M_p^3}\sqrt{\frac{f}{M'}}e^{\mu_\psi^2 N_{dens}/3} = 6.7 \times 10^{-6} \ , \tag{10}$$

while the model λ has the constraint:

$$\frac{\lambda e^{\mu_\psi^2 N_{dens}/3}}{\mu_\psi^2 \mu_\phi} = 1.6 \times 10^{-4} \ . \tag{11}$$

In the equations above, we defined $\mu_\psi = m_\psi/H$, and $\mu_\phi = m_\phi/H$; N_{dens} is the number of e-folds between the time at which the scales relevant for determining the density perturbations cross the horizon, and the time when $m_\phi(t) = 0$ at the origin. We will see in the next section, Eq. (41), how big exactly is this parameter N_{dens} for our models; these results will be more clear after the next section.

The exponential in Eqs. (10), and (11) determines the scale dependence of the density perturbations,

$$n = 1 - 2\alpha_s = 1 + \frac{2\mu_\psi^2}{3} \ . \tag{12}$$

This concludes the discussion about the scalar density perturbations. Conceivably, there could also exist tensor density perturbations that are due to the fact that the graviton field modes are conceivably excited in de Sitter space in a similar manner as the scalar perturbations are created [1]. However, it turns out that our models predict that the total energy stored in the graviton degrees of freedom will be negligible to the energy stored in the scalar perturbations, so we skip the derivation of the tensor perturbations, and refer the interested reader to [3] for this derivation.

4.3 Mathematical analysis of the number of e-folds

In this section, we provide the analysis for the M' model; the analysis for the second model is quite analogous, so we just state the result.

However, before going into the analysis of the number of e-folds, we have to say a few words about the decay of ψ into χ, which is a field of small mass coupled with ψ. Once the mass of ψ becomes large, the energy in ψ decays into relativistic χ particles, and decouples from the field ϕ.

We use two different models for the decay of ψ into χ. Each of these two decay mechanisms can be applied to either M' model, or λ model. For the explanation where the decay rates Γ come from please see [3]. In the first model, the decay rate is:

$$\Gamma_b \approx m_\psi(t) \ . \tag{13}$$

While ϕ is small, $\Gamma(t)$ is small also, and we can neglect the decay of ψ into χ. (Although we did take it into account in the computer simulations of the model development.) In the other model:

$$\Gamma_l \approx \frac{m_\psi^3(t)}{\left(M_P/\sqrt{(8\pi)}\right)^2} \ , \tag{14}$$

So, essentially, when ϕ becomes large enough, $\Gamma(t)$ for the decay of ψ into χ becomes significant compared to H, while $\Gamma(t)$ is still growing enormously. This makes the energy stored in ψ decay rapidly, and since for the parameters we are using, the oscillations in ψ are always bigger than $\Gamma(t)$, the fact that $\Gamma(t)$ is large does not slow down the propagation of ψ. In short, after the time $\Gamma(t)$ becomes comparable to H, we can forget about ψ very soon; the

fact that ψ is decreasing, in turn makes ϕ propagate much faster, thereby further increasing $m_\psi(t)$, and hence $\Gamma(t)$.

4.3.1 Stage 1

We define Stage 1 as the period during which ψ is slow-rolling towards the origin, and ϕ is small enough not to influence the propagation of ψ significantly.

Consequently, in this stage, the equation of motion of ψ is:

$$3H\dot{\psi} + m_\psi^2\psi = 0 \ . \tag{15}$$

In our models, the terms other than the constant make a negligible contribution to energy during the relevant last 40 e-folds of inflation. Therefore, H changes negligibly during inflation, and we can make the substitution: $N = Ht$, where N is the number of e-folds, and

$$H = \sqrt{\frac{8\pi}{3}}\frac{M^2}{M_P} \ . \tag{16}$$

Furthermore we define $N = 0$ at the moment when the mass squared of ϕ at the origin equals exactly zero, and N to be negative before that. Consequently, Eq. (15) becomes

$$3\frac{d\psi}{dN} + \mu_\psi^2\psi = 0 \ . \tag{17}$$

and, therefore:

$$\psi(N) = \psi_c e^{-\mu_\psi^2 N/3} \ . \tag{18}$$

where $\psi_c = \sqrt{2M'm_\phi}$.

At the same time, the equation of motion for ϕ is

$$3\frac{d\phi}{dN} - \mu_\phi^2\phi + \frac{\psi^4\phi}{4M'^2} = 0 \ . \tag{19}$$

In this equation, we assumed that ϕ is slow-rolling in Stage 1, which actually is not true, but is still a fairly good approximation; it gives the correct solution to within 1-3 e-folds. We checked this numerically as explained in the next section. Also, as will be clear from the definition of ϕ_c below, and

from the fact that $\psi \approx \psi_c$ throughout Stage 1, the term $\propto \phi^4\psi^2$ is negligible in Stage 1. Consequently, we did not include this term in Eq. (19).

Anyway, combining Eq. (19) and Eq. (18), and also using Taylor expansion in the exponential, we get:

$$\frac{d\phi}{dN} = \frac{4N\mu_\psi^2\mu_\phi^2}{9}\phi \ . \tag{20}$$

According to this equation

$$\phi(N) = \phi_i e^{2(N-N_0)^2/9w^2} \ , \tag{21}$$

where $w \equiv 1/\mu_\psi\mu_\phi$, ϕ_i is some initial value of ϕ, and N_0 is the number of e-folds when $\phi = \phi_i$. These two values are calculated from the fact that when the mass of ϕ at origin is small, the quantum fluctuations in ϕ dominate its classical evolution. This quantum development is described in [3]. The essential results are that

$$\phi_i = \sqrt{\frac{3}{4\pi}\sqrt{\frac{e}{\pi}}H^2 w} \tag{22}$$

and,

$$N_0 = w\sqrt{\frac{9}{8}} \ . \tag{23}$$

Stage 1 ends when ϕ becomes large enough to start influencing the development of ψ. This happens roughly when $\phi = \phi_c \equiv \sqrt{2M'H}$. So, we calculate the total number of e-folds N_1 in Stage 1 from Eq. (21) by setting $\phi_c = \phi(N_1)$. From this, we get our final answer for the number of e-folds in Stage 1 to be

$$N_1 \approx w\sqrt{\frac{9}{2}}\sqrt{\ln\left(\frac{\phi_c}{\phi_i}\right)} \ . \tag{24}$$

4.3.2 Stage 2

As explained above, at the end of Stage 1, ψ starts to oscillate rapidly, while its' amplitude decreases both because of H and Γ. Because the oscillations in ψ are very rapid compared to the development of ϕ for the parameters of

interest to us, we can approximate the development of ψ by the development of its envelope. The equation of development of amplitude of ψ is

$$\dot{\psi_e} = -\left(\frac{3H}{2} + \frac{\Gamma(t)}{2}\right)\psi_e \ . \tag{25}$$

Stage 2 is the stage of development of ϕ from the moment that ψ begins its' rapid oscillations till the moment when ψ decays into χ. Stage 2 therefore ends when $\Gamma(t) \approx H$.

According to our definition of Γ_b, for the first model of decay of ψ into χ, and ϕ_c, Stage 2 ends almost immediately after Stage 1 ends. Consequently, the total number of e-folds in Stage 2 for the Γ_b model, $N_2^b \approx 0$.

For the model of decay with Γ_l, we get that the Stage 2 ends when

$$\phi_l \approx \left(\frac{H M'^3 M_P^2}{\pi}\right)^{1/6} \ . \tag{26}$$

To calculate N_2^l, we note that it turns out that during Stage 2, the term $\propto \psi^4\phi^2$ is negligible, and that ϕ essentially keeps with the minimum of its potential which moves "right" as ψ red-shifts away. The potential we are talking about is therefore:

$$V = -\frac{m_\phi^2\phi^2}{2} + \frac{\phi^4\psi^2}{8M'^2} \ , \tag{27}$$

and from this potential,

$$\phi_l \equiv \phi(N_2^l) = \frac{\sqrt{2}m_\phi M'}{\psi(N_2^l)} = \sqrt{m_\phi M'}e^{3N_2^l/2} \ , \tag{28}$$

from which we conclude, using Eq. (25) and the fact that $\Gamma(t)$ is negligible during Stage 2, that

$$N_2^l = \left(\frac{1}{9}\right)\ln\left(\frac{M_P^2}{8H^2\pi}\right) \ . \tag{29}$$

We can also calculate the energy in χ at the end of Stage 2. We assume that all the energy that was stored in ψ particles at the end of Stage 2 is transfered into E_χ. Consequently, for Γ_b,

$$E^b_{\chi 2} \approx \frac{H^2 \psi_c^2}{2} \ , \tag{30}$$

and for Γ_l,

$$E^l_{\chi 2} \approx \frac{\phi_l^4 (\psi_c(N_2^l))^2}{8M'^2} \ . \tag{31}$$

4.3.3 Stage 3

Stage 3 is the period between the moment when $\psi \approx 0$ till the moment when ϕ begins its coherent oscillations around its true minimum.

Since ψ is gone, it does not influence the development of ϕ anymore. Furthermore, it turns out that all the terms of the potential in ϕ, other than the mass, and the constant term, are negligible all the way till the end. Therefore, the equation of motion of ϕ is approximately

$$\frac{d^2\phi}{dN^2} + 3\frac{d\phi}{dN} - \mu_\phi^2 \phi = 0 \ . \tag{32}$$

From the above equation it is clear that

$$\phi(N) = \{\phi_c, \phi_l\} e^{rN} \ , \tag{33}$$

depending on which model of decay we implement. We defined

$$r \equiv \sqrt{\mu_\phi^2 + \frac{9}{4}} - \frac{3}{2} \tag{34}$$

Using the above, and the fact that Stage 3 ends approximately when ϕ reaches its true minimum, we get

$$N_3 = \frac{1}{r} \ln \left(\frac{\phi_f}{\{\phi_c, \phi_l\}} \right) \ . \tag{35}$$

where ϕ_f is the final value of ϕ, that is the position of the true minimum of ϕ. Consequently, $\phi_f \equiv \pi/(f\sqrt{2})$.

Furthermore, we can calculate E_χ at the end of Stage 3 since we know that during Stage 3, the energy in the relativistic χ particles is redshifting away with $4H$; at the end of Stage 3, $E_\chi \approx E_{\chi 2} * e^{-4N_3}$.

4.3.4 Total number of e-folds

From the above, we conclude that, from the time the mass of ϕ at the origin equals exactly zero, till the time ϕ starts its rapid oscillations around its' true minimum, there are total of

$$N_{tot} \equiv N_0 + N_1 + N_2 + N_3 \tag{36}$$

e-folds, where N_2 and N_3 depend slightly on which model of decay we implement. However, it turns out, that in the end, N_{tot} for the two models of decay differs by only 3-5 e-folds.

The derivation for the model with Yukawa coupling is quite analogous, so we just state the results here. N_0 through N_3 are defined as for the first model, but, the ϕ's at which the stages end are slightly different;

$$\phi_c \equiv \frac{H\sqrt{2}}{\lambda} \ , \tag{37}$$

and,

$$\phi_l \equiv \left(\frac{M_P^2 H \sqrt{2}}{4\pi\lambda^3} \right)^{1/3} \ . \tag{38}$$

Some useful facts to have in mind when trying to develop the intuition for the development of the models is that $N_{tot} \uparrow$ when $\mu_\phi \downarrow$. This is so because a smaller μ_ϕ presents a flatter potential for ϕ. As we can see from the expression for N, $N_{tot} \propto 1/\mu_\phi$. In addition, N_{tot} decreases with an increase of μ_ψ as we can see from the expressions for N_0 and N_1. However, this dependence is much smaller.

This concludes our analysis of the number of e-folds after the time $N = 0$. We need this N_{tot} to determine which N goes into Eq.(10) and Eq.(11) to determine the density perturbations for the two models. The time when the relevant scales enter the horizon is given by [3]

$$N_{Mpc} = 38 + \frac{2}{3}\ln\left(\frac{M}{10^{11}GeV}\right) + \frac{1}{3}\ln\left(\frac{T_{RH}}{10^{7}GeV}\right) \ , \tag{39}$$

which for our models evaluates to

$$N_{Mpc} = 15.93 + \frac{2}{3}\ln\left(\frac{M}{1GeV}\right) + \frac{5}{18}\ln\left(\frac{m_\phi}{1GeV}\right) \ . \tag{40}$$

Consequently, the N which goes into the equations for determining the density perturbations is given by

$$N_{dens} \equiv N_{tot} - N_{Mpc} \ . \tag{41}$$

N_{dens} determined this way is 1-3 e-folds bigger than the true N_{dens} determined numerically as in the next section. Nevertheless, this is a small deviation, and we will use N_{dens} determined analytical way in all future calculations.

Unfortunately, the predictions for E_χ are not as great as the ones for N_{tot}; the mistake is anywhere between 10 and 10^4. However, it turns out that because of a big redshift, any initial E_χ at is typically many orders of magnitude smaller than the energy in ϕ particles at the time when these particles reheat the universe. Consequently, E_χ is irrelevant for the entire discussion. The only thing that we should worry about is that E_χ could maybe cause over production of gravitinos, but it turns out that we are safe from this danger also. All these facts are described in much more detail in [3].

4.4 Computer confirmation of the number of e-folds

The numerical simulations of the propagation of the models were done in MATLAB. Every stage above was developed separately, and the ending values of ϕ and ψ of one stage were taken to be the initial values for the next stage. We explored a wide range of values of different parameters that could conceivably be of interest to us. This convinced us that the analytical solution given in the previous section typically differed from the numerical one by 1-3 e-folds for all parameters of interest to us. Since this was a small deviation, we were allowed to use Eq. (41) above for all further calculations since this saved us enormous amount of time compared to using the numerical simulation for every set of parameters.

In this section, we describe the whole method, and give the codes, together with the results of propagation for one representative set of parameters which is illustrative how the method works. Again, the numerical calculation is used only as a check of the analytical expressions for N's of different stages, and the expressions for E_χ that are given in the previous section.

4.4.1 Stage 1

The program in MATLAB that solves numerically for the evolution of Stage 1 essentially solves the system of two coupled differential equation of second order in two variables ϕ, and ψ. The initial conditions are $\phi(0) = \phi_i$, $\psi(0) = \psi_c e^{-\mu_\psi^2 N_0/3}$, $\dot{\phi}(0) = 0$, and $\dot{\psi}(0) = 0$. The equations are given by:

$$\ddot{\phi} + 3H\dot{\phi} + \frac{\partial V(\psi, \phi)}{\partial \phi} = 0 \ , \tag{42}$$

and,

$$\ddot{\psi} + 3H\dot{\psi} + \frac{\partial V(\psi, \phi)}{\partial \psi} = 0 \ . \tag{43}$$

We propagate the above equations until the moment when ψ begins its rapid oscillations around its minimum. At this point, Stage 2 starts.

A typical development of this stage is given in Figure 1.

Once, ψ starts oscillating, we take its amplitude, as the initial condition for Stage 2. We also take the values of ϕ, and $\dot{\phi}$ as the initial conditions for Stage 2.

4.4.2 Stage 2

This simulation is also done in MATLAB. The equation for propagation of ϕ is the same as Eq. (42), but this time ψ is replaced by the envelope of its amplitude. It is oscillating too rapidly for MATLAB to be able to propagate it long enough. On the other hand, since it is oscillating so rapidly compared to the evolution of ϕ, the field ϕ effectively sees only the envelope of the amplitude of ψ. The evolution of envelope ψ_e is given by

$$\dot{\psi_e} = -\left(\frac{3H}{2} + \frac{\Gamma(t)}{2}\right)\psi_e \ . \tag{44}$$

Furthermore, it is trivial to calculate the total energy stored in ψ field;

$$E_\psi = \frac{\psi^4\phi^2 + \phi^4\psi^2}{8M'^2} \ . \tag{45}$$

Or, in the other model,

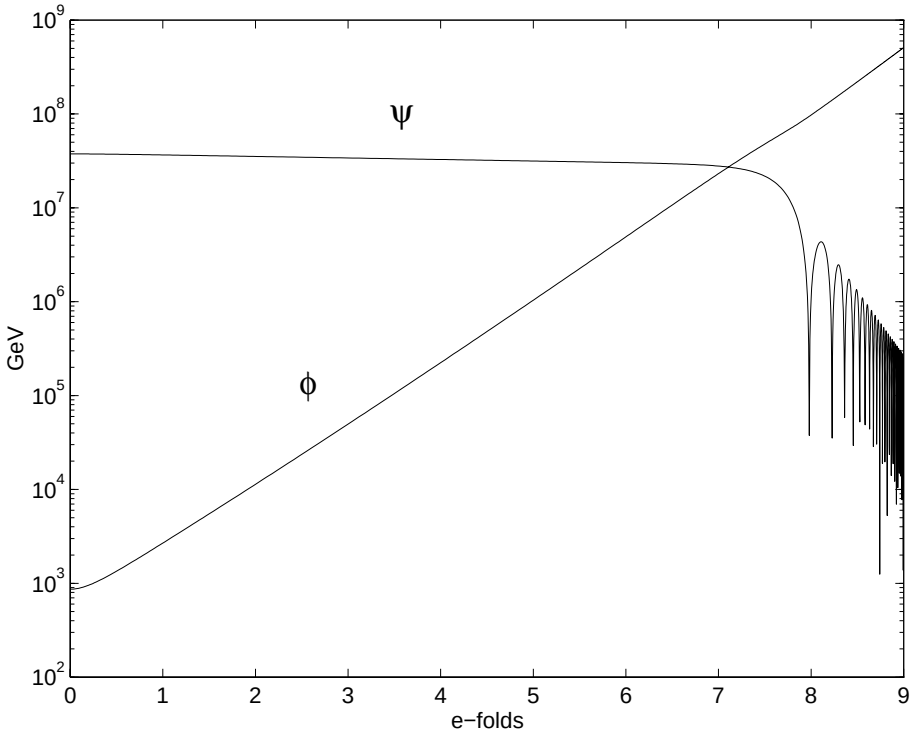

Figure 1: The numerical simulation for Stage 1. The example we choose is for M' model. We pick some typical values of the parameters: $\mu_\phi = 2.8$, $\mu_\psi = 1/3$, $M = 1.5 * 10^{11} GeV$, and $M' = 10^{11}$. Different parameters, or λ model differ only quantitatively.

$$E_\psi = \frac{\lambda^2 \psi^2 \phi^2}{4} \ . \tag{46}$$

We need to calculate E_ψ, because we want to calculate the total energy stored in χ as a function of time eventually. The equation for E_χ is

$$E_\chi = -4H + \Gamma(t) * E_\psi \ . \tag{47}$$

The factor $-4H$ is included because χ particles are relativistic, so they red-shift with $4H$. A continuation of the propagation of the parameters of Figure 1 is shown in Figure 2.

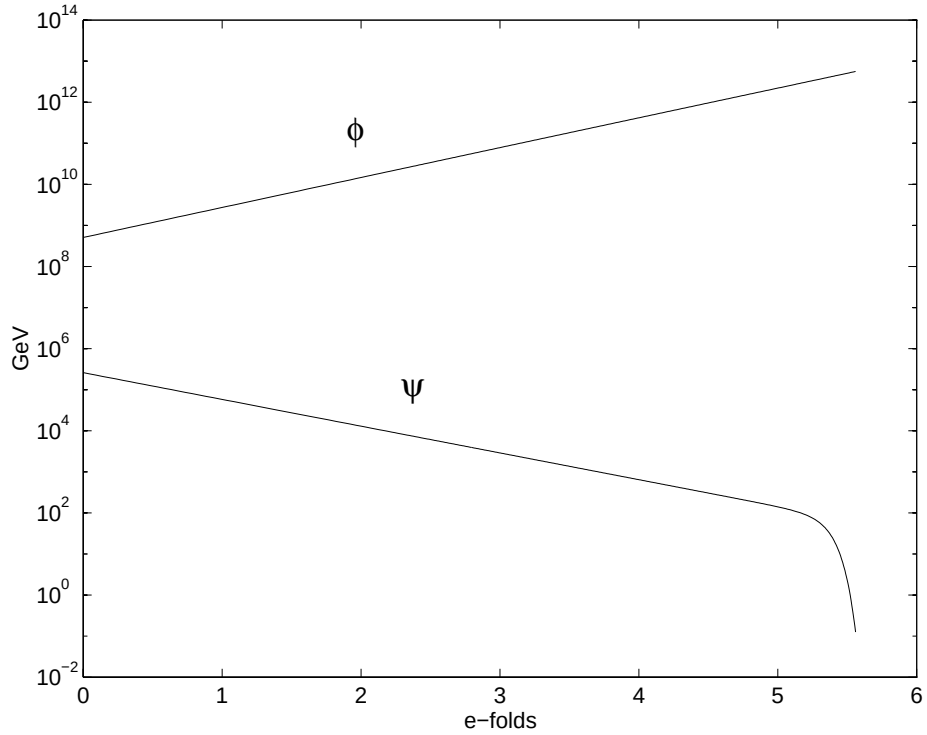

Figure 2: The numerical simulation for the development of ϕ, and the envelope of ψ in Stage 2. All the parameters are as for Figure 1. This particular example is for the model with Γ_l.

As we said, we also use MATLAB to calculate the propagation of E_χ; the result corresponding to the development of ϕ, shown in Figure 2 is shown in Figure 3.

This concludes our simulation for Stage 2. The continuation of the development of the model is done in the next section. We take the final values of ϕ, $\dot{\phi}$, and E_χ as the initial values for Stage 3.

4.4.3 Stage 3

Stage 3 is the numerical simulation of the development of the model once E_ψ is too small to influence the development of ϕ or E_χ in any way. Consequently, we set $\psi_e \equiv 0$, and use the equations of the previous section to propagate

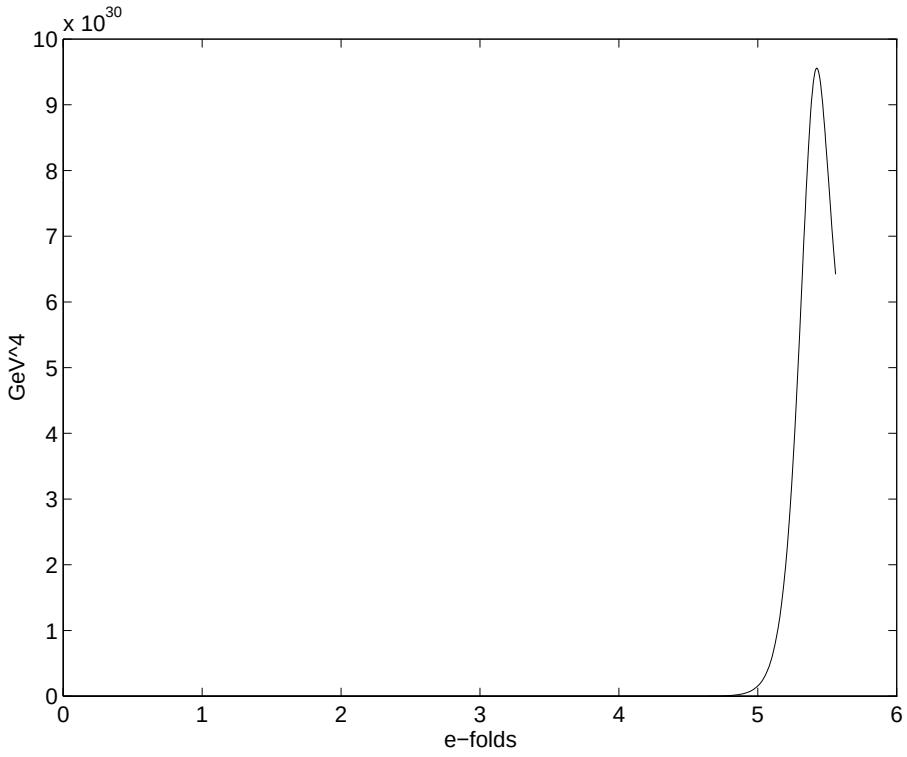

Figure 3: The numerical simulation for the development of E_χ in Stage 2, corresponding to the development of ϕ, and ψ_e shown in Figure 2.

the model further. Obviously, in these equations, $E_\psi = 0$ now. The result of the simulation is shown in Figures 4, and 5.

This concludes the whole development, till the point when ϕ starts to oscillate. The numerical simulations of many examples of different parameters prove that our analytical expressions were rather good, and that we are justified in using them for the further exploring of the models.

4.5 The spike in the density perturbations

As we said before, when $m_\phi \approx 0$, the quantum fluctuations dominate the development of ϕ. It turns out that this feature of our models results in a large energy density perturbations which should conceivably be observable at the scales that enter the horizon while $m_\phi \approx 0$. We calculate the exact

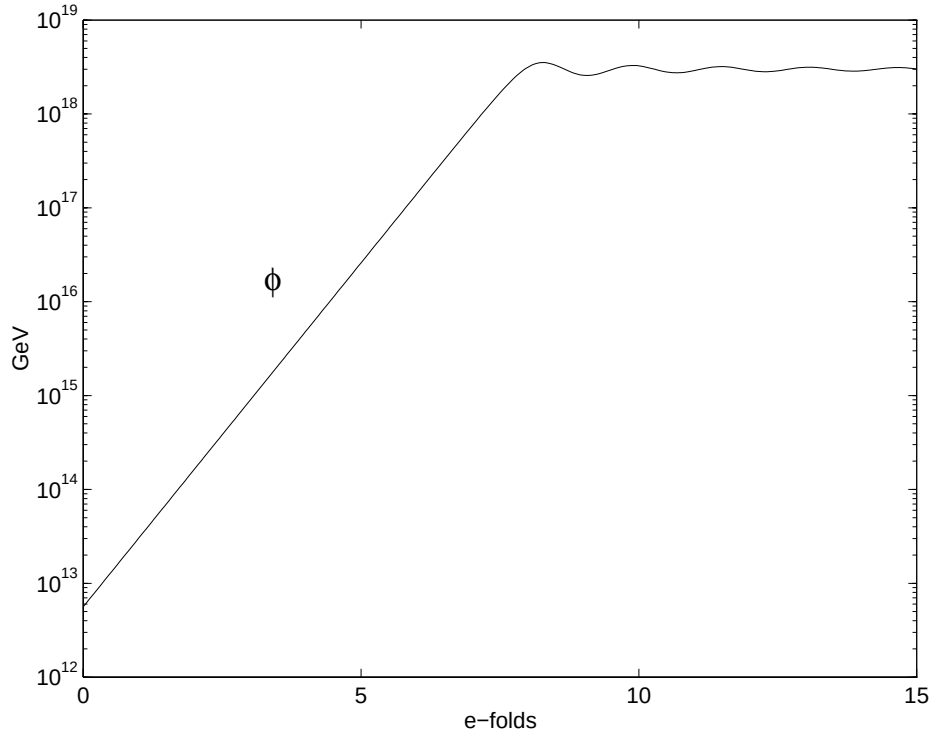

Figure 4: The numerical simulation for the development of ϕ in Stage 3. All the parameters are as for Figure 1. This is just a continuation of Stage 2; $\psi \equiv 0$ here.

shape of these perturbations in [3]. They look approximately like a gaussian of width $\approx w$, and maximum height ≈ 1.

This spike is a characteristic of our models that should conceivably distinguish it from the predictions of the other models one day the relevant scales become observable. However the scales observable today through CMBR have density perturbations much smaller than 1, as we said before. Consequently, we have to make sure to "put" this spike in the scales unobservable today. We showed in [3] that if the peak of the spike is at more than $5w$ e-folds smaller scales than 1Mpc, its contribution to the density perturbations are negligible, and we can use the formulas from Section 4.2. to determine the density perturbations.

Consequently, in our calculations, we have to make sure that the scales

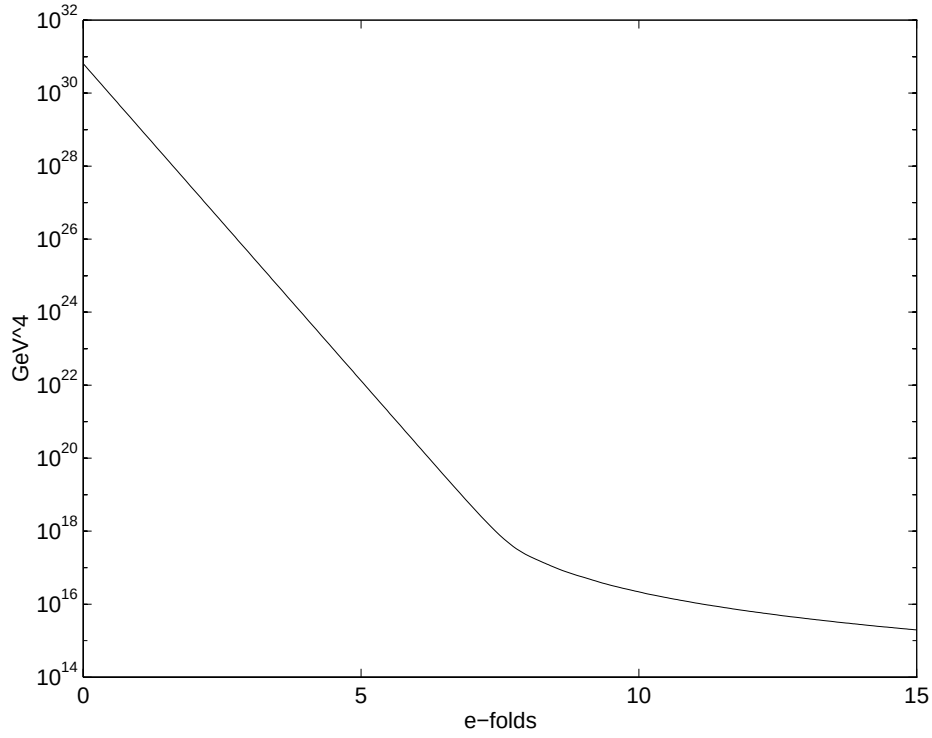

Figure 5: The numerical simulation for the development of E_χ in Stage 3, corresponding to the development of ϕ shown in Figure 4.

that determine the density perturbations are at least $5w$ away from the point when $\psi = \psi_c$ because that point is the peak in the spike. In other words, we impose the requirement

$$N_{dens} \leq -5w \ . \tag{48}$$

4.6 Creating the plots of masses

Our main goal in this project was to develop a model which will not incorporate any new inexplainable small parameters; it will perform inflation using only the natural, already existing parameters.

In the case of our models the requirement of naturalness means that all weak mass scales should be of order H, meaning $\mu_\psi \approx 1$, and $\mu_\phi \approx 1$. In

addition, the mass M should be of order $M_I \approx 10^{11} GeV$, and the fact that m_ϕ, and m_ψ are at weak scale, means that we would like them to be of the order $10^2 - 10^4 GeV$.

The most natural values of m_ϕ, and m_ψ we were able to obtain are presented as functions of given M in Figures 6-9. The reader can pick a value of M they consider to be most natural, and the most natural other parameters obtainable, given the constraints of our models, and the picked value of M, can be read off the plots. All the plots are for Γ_b.

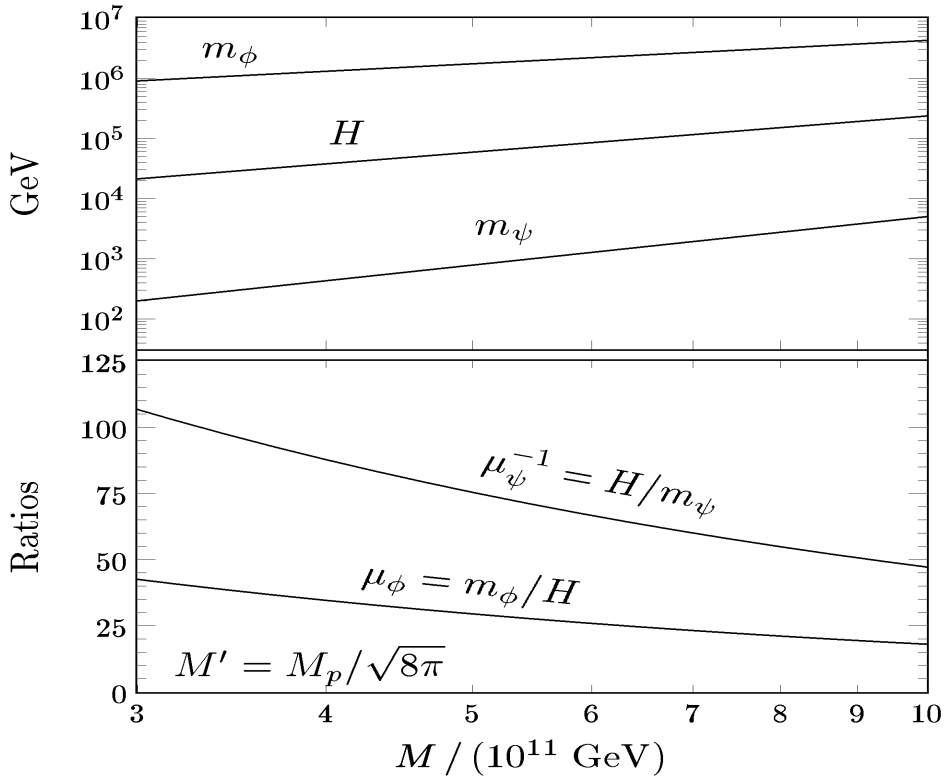

Figure 6: This Figure presents the result of optimizing our M' model, with M' at the Planck scale, given the constraints of the density perturbations, and the constraining spike in the density perturbations.

As we said, $N_{tot} \uparrow \Leftrightarrow \mu_\phi \downarrow$. Consequently, we want to have N_{tot} as large

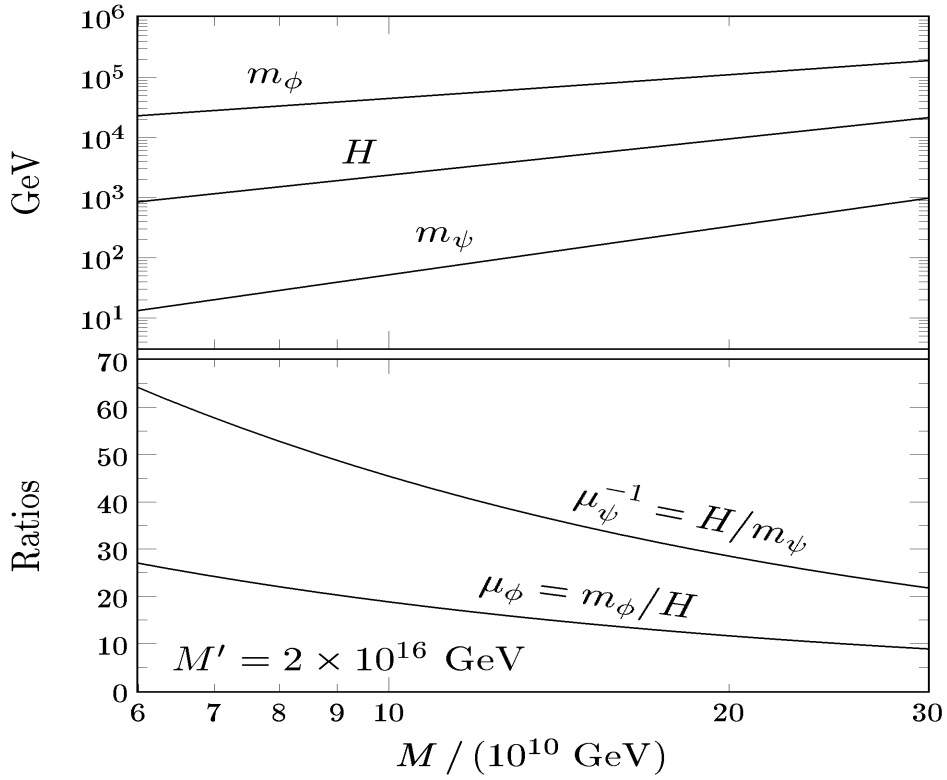

Figure 7: This Figure presents the result of optimizing our M' model, with M' at the GUT scale, given the constraints of the density perturbations, and the constraining spike in the density perturbations.

as possible. But, we have to obey the constraint given by Eq. (41), and Eq. (48). Therefore, the best we can do is if we impose the requirement on our parameters such that they result in

$$N_{dens} \equiv -5w \ . \tag{49}$$

The other constraints that we have to obey are given by Eq. (10), or alternatively, Eq. (11). The fact that we are determining μ_ψ once μ_ϕ was imposed to be as small as possible is a good strategy because the density perturbations are determined more strongly with μ_ψ than with μ_ϕ, while

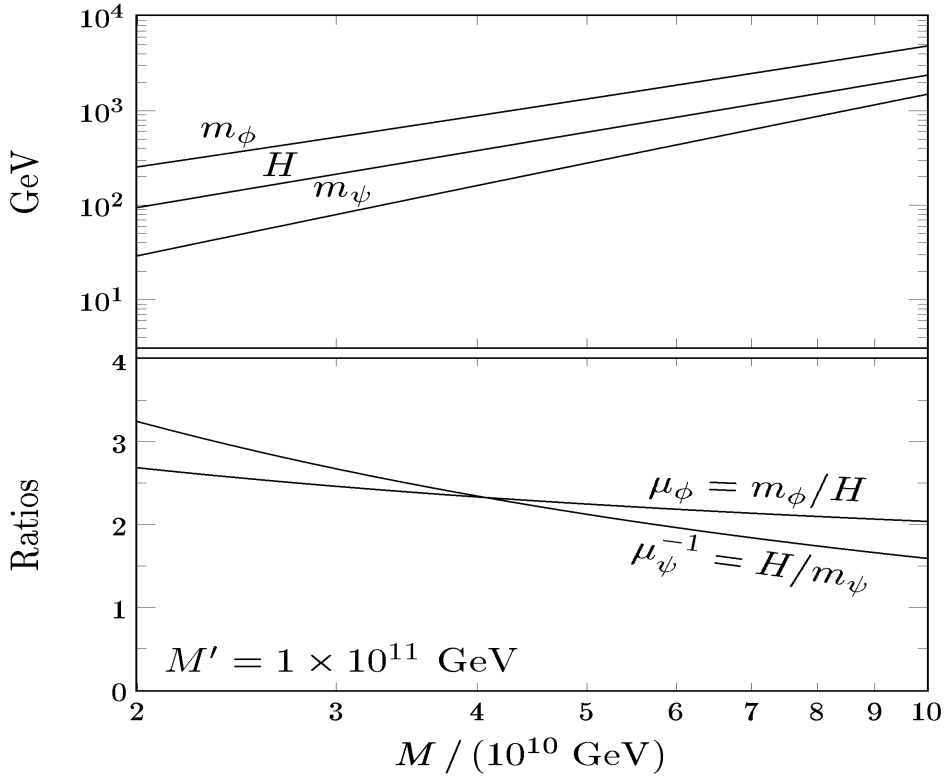

Figure 8: This Figure presents the result of optimizing our M' model, with M' at the intermediate scale, given the constraints of the density perturbations, and the constraining spike in the density perturbations.

N_{dens} depends more strongly on μ_ϕ. So, the two variables are virtually decoupled, and we can optimize them almost separately.

This procedure yields the best values μ_ψ, and μ_ϕ, as a function of the other parameters that are inputs to our models.

We wrote a program to implement this procedure; a typical example of the program is given in the appendix. For every value of M, the program finds the optimal values of μ_ψ and μ_ϕ. So, for a vector of variables M, it returns a vector of the corresponding optimal μ_ϕ, and μ_ψ. These vectors are then used to create the plots of masses in Figures 6-9. The plots are a result

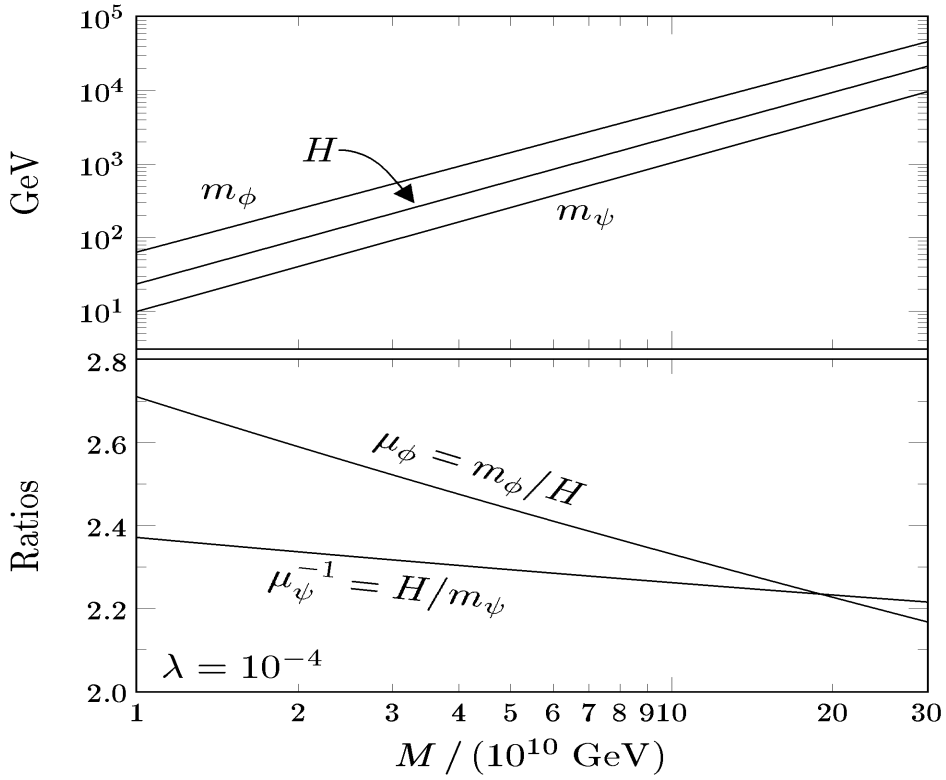

Figure 9: This Figure presents the result of optimizing our model with the Yukawa coupling, with $\lambda = 10^{-4}$, given the constraints of the density perturbations, and the constraining spike in the density perturbations.

of the optimization of our model; they are the most natural parameters our models can feasibly use.

As explained above, all the plots, and the program are for Γ_b. We mentioned above the the models with Γ_l typically propagate for 3-5 e-folds more, so their parameters would look a bit worse, but not much more so. Nevertheless, they would be quite the same qualitatively.

4.6.1 Description of the program

The program in the appendix is for the model with the Yukawa coupling. The program used to calculate the parameters for M' model is quite analogous.

The idea of the program is to search iteratively for the values of μ_ψ, and μ_ϕ till both parameters are obtained with the specified precision. In this section we give a brief description of each procedure. The reader should then have no problem to analyze and understand the code.

Procedure **main** defines the main parameters. In addition, it calls the procedures that calculate the optimal parameters for every M required to calculate it for. Furthermore, it sets up the initial values for the iteration. Finally it outputs the vectors of M, and the corresponding calculated values of the masses.

Procedure **find-h** just returns the value of H given M.

Procedure **density-pert** takes as inputs μ_ψ, and μ_ϕ, and returns the value of the density perturbations that would result from such parameters.

Procedure **n-e-fold-anal** takes as inputs μ_ψ, and μ_ϕ, and returns analytical value of $N_{dens} + 5w$; this is the value we would like to constrain to zero according to Eq. (49).

The first procedure that does some minimizing work is **find-mu-psi** which takes μ_ϕ as given, and finds the value of μ_ψ to satisfy the density perturbations constraint given M, and μ_ϕ.

Similarly, the procedure **find-mu-phi** takes μ_ψ as given, and finds the value of μ_ϕ to satisfy Eq. (49) given M and μ_ψ.

The final procedure, that does all the work of finding μ_ψ and μ_ϕ for each M it is called with, is called **itterate**. It takes an initial value of μ_ϕ. Given this μ_ϕ it finds the μ_ψ to satisfy the density constraint. It does so using **find-mu-psi**. Next, it uses the μ_ψ calculated this way to find μ_ϕ needed to satisfy Eq. (49) given μ_ψ. It does so using **find-mu-phi**. Given this μ_ϕ it finds the μ_ψ to satisfy the density constraint. Etc. till the required precision is satisfied after many iterative steps.

5 Conclusion

As the reader can see from Figures 6-9, the resulting values of the masses are excellent. We have achieved our initial goal; our models do not incorporate any new small parameters. Instead, they implement inflation correctly using only the parameters already existing in the particle physics theories.

One of the distinguishing predictions of our models is that the scalar index n is very close to 1, but in general slightly bigger; this is clear from Eq. (12), and from Figures 6-9. Furthermore, there is a characteristic spike in the density perturbations at so far unobservable scales. In addition, our models predicts that the tensor perturbations are negligible. For further implications of our models, please see [3].

6 Acknowledgements

The work was done under the guidance, and supervision of Professor Lisa Randall, and Professor Alan Guth. I am extremely grateful to them for making this project possible, and for all of their help and guidance.

We are very grateful to Andrew Liddle, David Lyth, and Ewan Stewart for discussions and the Aspen Center for Physics where these discussions took place. We also thank Sean Carroll, Csaba Csáki, Arthur Kosowsky, Andrei Linde, and Bharat Ratra for their comments. We thank Bernard Carr, Jim Lidsey, Avi Loeb, Paul Schechter, and Paul Steinhardt for discussions and correspondence about black holes. We also thank Krishna Rajagopal for his comments on the manuscript.

The work of L.R. was supported in part by the Department of Energy under cooperative agreement DE-FC02-94ER40818, NSF grant PHY89-04035, NSF Young Investigator Award, Alfred Sloan Foundation Fellowship, and DOE Outstanding Junior Investigator Award. The work of M.S. was supported in part by MIT UROP. The work of A.H.G. was supported in part by the Department of Energy under cooperative agreement DE-FC02-94ER40818.

References

[1] E. W. Kolb and M. S. Turner, The Early Universe (Addison-Wesley Publishing Company, USA 1994).

[2] A. D. Linde, Particle Physics and Inflationary Cosmology (Harwood Academic, Switzerland, 1990).

[3] L. Randall, M. Soljačić, and A. H. Guth, MIT preprint CTP #2501, hep-ph/9512439.

[4] A. Guth and S.-Y. Pi, Phys. Rev. Lett. **49**, 1110 (1982); A. Starobinsky, Phys. Lett. **117B**, 175 (1982); S. Hawking, Phys. Lett. **115B**, 295 (1982); J. Bardeen, P. Steinhardt, and M. Turner, Phys. Rev. D **28**, 679 (1983).

[5] A. R. Liddle and D. H. Lyth, astro-ph/9409077.

[6] A. Guth, Phys. Rev. D **23**, 347 (1981).

[7] G. Smoot et al., *Ap.* J. **396**, L1 (1992); E. L. Wright et al., *ibid*, L13 (1992).

[8] C. B. Collins and S. W. Hawking, *Ap.* J. **180**, 317 (1973).